A Compact Log Periodic Planar Dipole UHF Array Sensor for Partial Discharge Measurements

Meka Kalyan Chakravarthi, A. V. Giridhar, *Senior Member, IEEE*, Gande Arun Kumar, *Senior Member, IEEE*, and D. V. S. S. Siva Sarma, *Senior Member, IEEE*

***Abstract*—A compact log periodic planar dipole UHF array antenna from 500 MHz to 2.2 GHz for partial discharge measurement in power transformers is presented in this paper. The compactness of the designed antenna is achieved by shaping the arms and tuning selected dipole elements of the array to fill the unoccupied areas. Shaped dipole arrangement results in additional capacitance between the antenna elements enhancing the bandwidth. The designed antenna achieves a fractional bandwidth of 126% and the size is ($0.495\lambda_0 \times 0.63\lambda_0 \times 0.0144\lambda_0$) at center frequency of 1.35 GHz. The proposed antenna is experimentally validated on FR4 3.2 mm thickness substrate. The measured gain of antenna is 4 $\pm$ 0.5 dBi over 800 MHz to 2.2 GHz which provides lower variation in measured partial discharges. The effective antenna height of the proposed antenna is measured to be over 15 mm. The measured return loss is better than 10 dB over the frequency range. Moreover, partial discharge measurements with oil filled test objects demonstrate that the designed antenna can receive partial discharge signals effectively.**

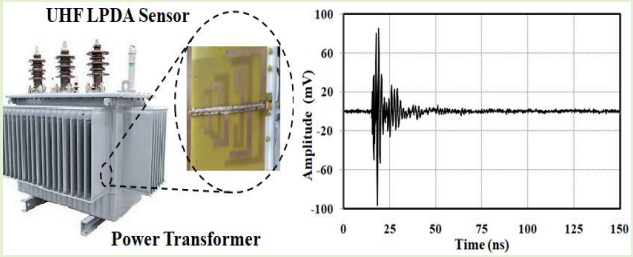

***Index Terms*—Fractional bandwidth, linear dipole antenna array, partial discharge, ultra high frequency sensor, ultra wideband antennas.**

I. Introduction

WITH the rapid growth of electricity in developing countries like India, cost effective production of electricity with equipment of higher power ratings is essential. This equipment should be insulated to provide reliable and safe service in compact sizes. Due to continuous operation of this equipment, sudden failure and outages occur as the insulation deteriorates with time. Hence, continuous quality monitoring of the insulation in this power equipment is essential in the power system operation and the most popular assessment is identification of partial discharges.

Partial Discharge (PD) is the dominant diagnostic quantity that manifests incipient discharges in the transformer. Recently, researchers have been focusing on detecting the PD's using radio frequency methods, as it provides improved sensitivity and vigorous anti interferences [1]. For any kind of PD antenna design, the effectiveness and ability of the antenna for monitoring the condition of the equipment is given by the effective antenna height which is the figure of merit for the sensor [2]; Though, the PD discharge frequency range is from 0.3 GHz to 3 GHz, however, the criticality in compactness of antenna design is due to lower frequency range requirement for PD i.e. from 0.3 GHz to 1 GHz.

The important sensors used in radio frequency (RF) method are broad band antennas. A RF antenna in the frequency range of 0.5 GHz to 2 GHz is employed for detecting PDs and also for examination of transformer oil [3]. In [4], the performance of three different RF antennas i.e.; dipole, axial helix and circular loop are compared with the commercial acoustic sensor for detection of PD signals. The designing of Ultra high frequency (UHF) sensor using FDTD simulation tool is demonstrated and its performance is tested in [5]. Various broadband antennas such as different shaped monopole, spiral, and loop antenna are used as sensors for PD detection in power transformer [6]. A dual slot barrier sensor [7] is designed for PD detection in gas insulated substation apparatus and working from 1 GHz to 2.6 GHz frequency range.

Several antennas are used for wideband performances such as bow tie antennas, Vivaldi antennas and Archimedean spiral antennas. In [8], the Archimedean antenna performance is

Manuscript received August 27, 2021; revised October 13, 2021; accepted October 14, 2021. Date of publication October 29, 2021; date of current version December 14, 2021. The associate editor coordinating the review of this article and approving it for publication was Prof. Piotr J. Samczynski. *(Corresponding author: Meka Kalyan Chakravarthi.)*

Meka Kalyan Chakravarthi, A. V. Giridhar, and D. V. S. S. Siva Sarma are with the Department of Electrical Engineering, National Institute of Technology, Warangal, Telangana 506004, India (e-mail: kalyan.mvr@gmail.com; giridhar@nitw.ac.in; dvss@nitw.ac.in).

Gande Arun Kumar is with the Department of Electronics and Communication Engineering, National Institute of Technology, Warangal, Telangana 506004, India (e-mail: g.arun@nitw.ac.in).

Digital Object Identifier 10.1109/JSEN.2021.3124418

analyzed for different types of PD defects. Bow tie antennas are non-planar structures whereas spiral and Vivaldi antennas are planar structure but all these antennas are not compact. The feeding is also very complex for these antennas as balun is required which further increases cost and complexity during the integration of other components of the system. Fractals such as Hilbert, stacked Hilbert, Sierpinski, and Koch structures are used for miniaturization of these antennas. However, the radiation pattern of these antennas have to be oriented for proper measurement of the PDs. Printed log periodic dipole antenna exhibits broad bandwidth characteristics with compact dimensions. As the antenna is in planar form, its integration with other circuit components is easy. Since, these antennas are specifically used for PD measurements they have to be small, compact and provide end-fire radiation for proper measurement of PD faults in the transformers [9]–[13].

In [14], a thirty element log periodic dipole array (LPDA) type optical electric field sensor (OEFS) is designed for computing the electromagnetic field interferences which operates in the frequency range of 1.8 to 6 GHz. The antenna provides a fractional bandwidth (FBW) of 107.69% with the dimensions of $1.391\lambda_0 \times 0.91\lambda_0 \times 0.195\lambda_0$(L × W × H) and λ_0 is the wavelength at center frequency. Though the sensitivity of the OEFS sensor is highly desirable and minimum detectable electric field strength at 2 GHz is 70 μV/m at 1 MHz resolution bandwidth, however the complexity of the antenna increases with the use of $LiNbO_3$ optical waveguide and the antenna also uses high dielectric constant substrate which results in feeding line losses. A low profile log periodic monopole array consists of 15 monopole hats of elliptical shape is designed which operates from 1.5 - 6.8 GHz frequency range [15]. The antenna provides a fractional bandwidth of 127.7% occupying a size ($5.81\lambda_0 \times 5.81\lambda_0 \times 0.0032\lambda_0$), however, the structure is complex as it contains top hat monopole in a multi-layer printed circuit board configuration. In [16], a miniaturized log periodic dipole array antenna is designed with complementary split ring resonators consisting of eighteen dipoles working from 0.4 - 1.8 GHz frequency range ($1.35\lambda_0 \times 1.1\lambda_0 \times 0.008\lambda_0$) with 127.3 % FBW and the size is large. A reconfigurable printed log periodic dipole array (RPLPDA) antenna consisting of eight dipoles on FR4 substrate is designed in [17] and the diverse frequency bands over a wide frequency range can be yielded by switching the eight printed dipoles. The RPLPDA covers frequency range of 0.75 - 2.7 GHz within size of ($1.093\lambda_0 \times 0.863\lambda_0 \times 0.0092\lambda_0$) with 113% FBW.

A wideband spiral shaped coupler consists of tuning nodules is developed for detection of PD's [18]. The UHF coupler size is ($1.033\lambda_0 \times 1.033\lambda_0 \times 0.0155\lambda_0$) with 135.5% FBW and working from 0.5 - 2.6 GHz frequency range with peak gain of 4.8 dB. Though, the FBW is good, the antenna is not compact, moreover the gain for the antenna fall at higher frequencies resulting in variation of measured PDs. The Archimedes Spiral Antenna (ASA) is particularly designed for detection of PD in rotating machines [19]. The ASA size is ($0.842\lambda_0 \times 0.842\lambda_0 \times 0.008\lambda_0$) with 120% FBW and from 0.5-2 GHz bandwidth with simulated gain of −11 to 3 dB.

An integrated sensor is fabricated by placing a fluorescent fiber optic on the disc UHF sensor top surface for GIS application [20]. The sensor size is ($0.5\lambda_0 \times 0.5\lambda_0 \times 0.006\lambda_0$) with 100% FBW and operates from 0.5 - 1.5 GHz with sensitivity of 8 mm. An ultra-wideband Metal Mountable Antenna (MMA) is designed for PD detection in contaminated insulator [21]. The MMA size is ($1.598\lambda_0 \times 1.37\lambda_0 \times 0.05\lambda_0$) with 152.94% FBW and works from 0.4 - 3 GHz bandwidth exhibiting a gain from −5.2 to −10.5 dBi. A circular printed monopole antenna is designed for PD detection in oil cell [22]. The antenna size is ($0.9\lambda_0 \times 0.9\lambda_0 \times 0.013\lambda_0$) with 130% FBW and operates over 0.3 - 1.5 GHz with S11 less than −10 dB. The simulated gain of the antenna is −1 to 5 dBi.

Compact LPDA have been designed by loading single and double T-shaped structures, dielectric loading with sinusoidal curves, dual band dipole and radial stubs [23]–[27]. However, FBW and frequency range of these antennas are not sufficient for PD measurements. The comparison of various parameters of the reported antennas is shown in table I.

TABLE I
PERFORMANCE COMPARISON OF DESIGNED ANTENNA WITH OTHER REPORTED ANTENNAS IN THE LITERATURE

Ref	Dimension (LxW) (mm)	Antenna Size (Area)	Freq. range (GHz)	Gain (dBi)	S_{11} (dB)	FBW (%)	Eff. Ant. Ht. (mm)
[7]	190 x 60	$1.14\lambda_0$ x $0.36\lambda_0$ ($0.41\ \lambda_0^2$)	1.0 – 2.6	-	-6	88.9	> 13
[16]	368 x 300	$1.35\lambda_0$ x $1.1\lambda_0$ ($1.49\lambda_0^2$)	0.4 – 1.8	-3 to 1.8	-10	127.3	-
[18]	200 x 200	$1.03\lambda_0$ x $1.03\lambda_0$ ($1.07\ \lambda_0^2$)	0.5 – 2.6	0-4.8	9.55	135.5	-
[19]	202 x 202	$0.84\lambda_0$ x $0.84\lambda_0$ ($0.71\ \lambda_0^2$)	0.5 – 2.0	-11 to 8*	-10	120	-
[20]	150 x 150	$0.5\lambda_0$ x $0.5\lambda_0$ ($0.25\ \lambda_0^2$)	0.5 – 1.5	-	-	100	8
[21]	282 x 242	$1.59\lambda_0$ x $1.37\lambda_0$ ($2.19\ \lambda_0^2$)	0.4 – 3.0	-5 to -11	-10	152.9	-
[22]	300 x 300	$0.9\lambda_0$ x $0.9\lambda_0$ ($0.81\ \lambda_0^2$)	0.3 – 1.5	-1 to 5*	-10	130	-
[23]	154 x 84	$0.77\lambda_0$ x $0.42\lambda_0$ ($0.32\ \lambda_0^2$)	0.8 – 2.2	2 to 6	-10	87.3	-
[24]	420 x 577	$0.70\lambda_0$ x $0.97\lambda_0$ ($0.68\ \lambda_0^2$)	0.2 - 0.8	3.2 to 5.5	-10	120.2	-
[25]	260 x 218	$3.45\lambda_0$ x $4.17\lambda_0$ ($14.39\ \lambda_0^2$)	0.5 - 10	3 to 6	-10	181	
This work	110 x 140	$0.495\lambda_0$ x $0.63\lambda_0$ ($0.31\lambda_0^2$)	0.7 – 2.2	-1 to 5	-10	126	> 15

* Simulated results. λ_0 Is the wavelength at centre frequency.
Eff. Ant. Ht. is Effective Antenna Height

The effect of transformer tank on the PD measurements is experimentally validated and their accurate simulation models are presented in [28] and [29]. The PD acquisition depends on antenna frequency response, tank enclosure resonance modes, and frequency content distribution of PDs [28]. The amplitude and cumulative energy of EM waves are accurately modeled using CST simulations and experimentally validated. It is concluded from the results that amplitude and cumulative energy of EM waves inside a transformer decrease non-linearly and the energy increases at lower frequencies however, attenuation is greater and energy ratio is less at higher frequencies [29].

In this paper, a seven element log periodic dipole array antenna is designed and validated. The structure is modified by selectively optimizing the elements of the array and the dipoles are shaped to provide additional capacitance which results in overall size reduction and flat gain performance. The coupling capacitance between the dipoles improves low

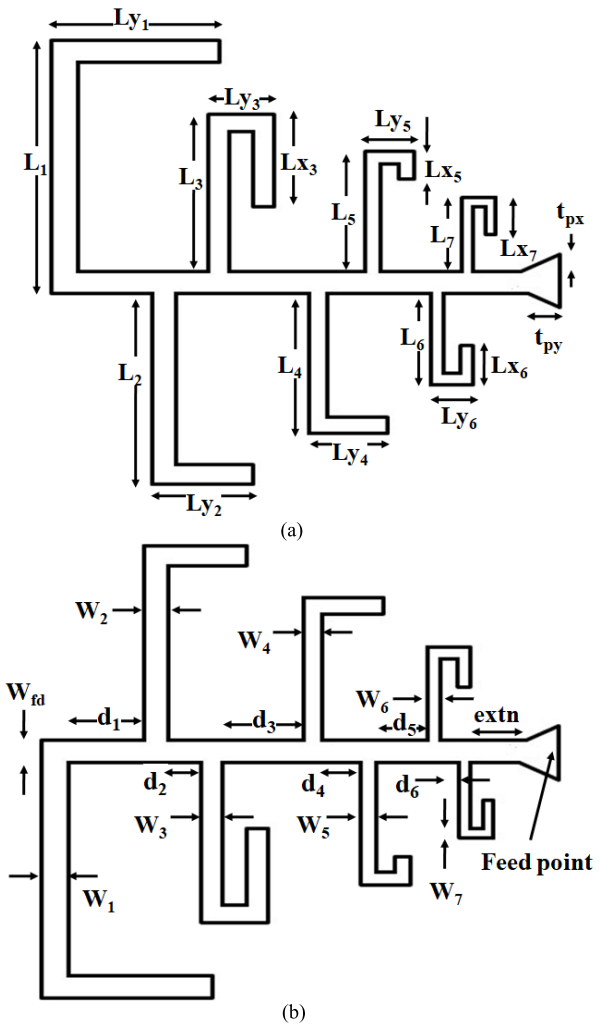

Fig. 1. a. Top layer of the proposed LPDA UHF sensor. b. Bottom layer of the proposed LPDA UHF sensor.

frequency bandwidth and matching due to increase in electrical length of dipoles. The measured fractional bandwidth for the antenna is 126 % in a compact area of 110 mm × 140 mm ($0.495\lambda_0 \times 0.63\lambda_0$). Section II of the paper presents the proposed antenna structure and its design process. Parametric study and analysis of the important dimensions of the LPDA are presented in Section III. Section IV discusses the measured results of the antenna and experimental setup for partial discharge measurement. The conclusions of the present research are presented in Section V.

II. Antenna Structure and Design

The log periodic dipole array antenna with seven dipole elements is shown in Fig. 1. The planar dipoles are arranged on top and bottom copper layers of the FR4 substrate with a dielectric constant of 4.4 and substrate thickness of 3.2 mm. The initial elements are designed based on Carrel table for the log periodic antenna [30]. The length of the dipole (L), distance between the elements (d) and the width of the dipoles (W) are varied logarithmically to achieve wide bandwidths and flat gain performance for the antenna array. Traditionally, this method is used for UHF and VHF antennas to achieve broadband characteristics. Since, the dipole structure is on

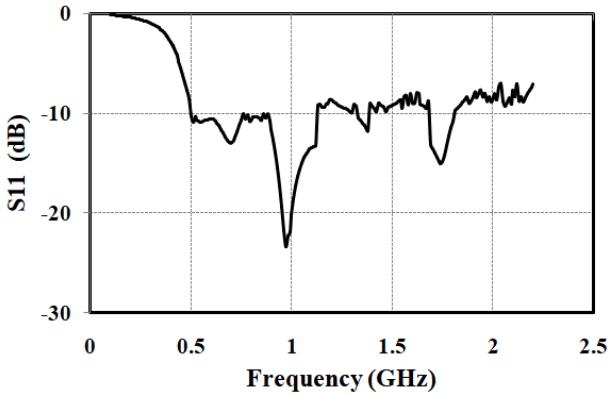

Fig. 2. Simulated S_{11} of the initial LPDA UHF sensor.

either side of the substrate, it results in a single back lobe radiation, as back lobe radiation is dependent on the angle between the dipole arrays. The basic principle and mathematical analysis are presented here for completeness. The geometry constant (τ), angle (α) and space constant (σ) are defined as in equation (1) and (2)

$$\frac{1}{\tau} = \frac{W_{k+1}}{W_k} = \frac{L_{k+1}}{L_k} = \frac{d_{k+1}}{d_k} \tag{1}$$

$$\alpha = \tan^{-1}\left(\frac{1-\tau}{4\sigma}\right) \tag{2}$$

where W_{k+1}, L_{k+1} and d_{k+1} (the subscript k = 1, 2, ...N-1 and N is the number of the dipoles) are the width, length and distance between the elements for the $(k+1)^{th}$ element and W_k, L_k and d_k are the width, length and distance between the elements for the k^{th} element. $(k+1)^{th}$ element is the largest dipole element.

The dipoles are resonant at their corresponding half wavelengths. The bandwidth depends up on the values of τ and σ, the required number of dipole elements are high, if the value of τ is high and the length of antenna increases, if the value of σ is small. Hence, to keep the antenna to a reasonable length the values of τ and σ are chosen to be 0.78 and 0.14, respectively. The number of dipole elements selected is seven instead of eleven to achieve the required bandwidth. The largest dipole and its adjacent dipole are shaped to be parallel so that a coupling capacitance is obtained between these dipoles due to electric fields. This additional capacitance results in increase of the electrical lengths of the dipoles. Thus, improving low frequency return loss performance of the LPDA. The substrate height and width of the feed line is chosen so that the input impedance of the line is 50 Ohms. This is achieved using taper lines at the coaxial to microstrip transition. This improves the return loss of the antenna. Coaxial feed is chosen in this design to simplify the feed mechanism by eliminating the balun structure which performs impedance match between the antenna and the feed. The match between the port impedance of 50 Ohms and input impedance for initial LPDA antenna is substantiated by plotting the S11 as shown in Fig. 2. The initial design values are obtained from the equation (1) and (2). The selection of the dipole elements for improving the return loss performance of the antenna array are L_1, L_2 and L_5 as the return loss represented by S11 in dB at the mid-band frequencies (i.e. 1.2 GHz to 1.7 GHz) and at 2 GHz

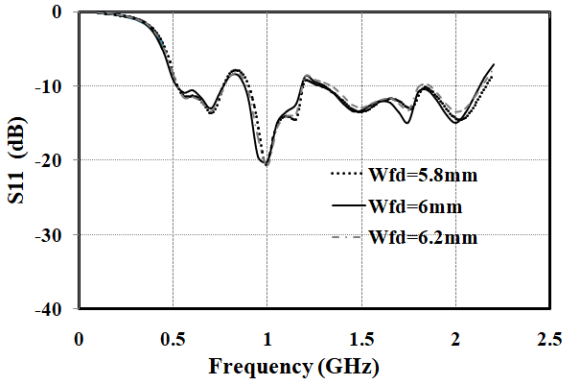

Fig. 3. Simulated S11 for variation in feed width of the antenna.

TABLE II
DIMENSIONS OF THE DESIGNED ANTENNA STRUCTURE IN MILLIMETERS

L_1	L_2	L_3	L_4	L_5	L_6	L_7	Ly_1	Ly_2
42	35	27	23	18	14	9.5	50	28
Ly_3	Ly_4	Ly_5	Ly_6	Ly_7	Lx_3	Lx_4	Lx_5	Lx_6
7	12	9	6	4	22	6	7	6
Lx_7	W_1	W_2	W_3	W_4	W_5	W_6	W_7	W_{fd}
5.2	6.5	6	5.4	6.5	4.2	2.8	1.8	6
d_1	d_2	d_3	d_4	d_5	d_6	extn	t_{px}	t_{py}
15	10	20	12	13	9.6	15	1.4	15

is poor compared to other frequencies. The dimensions of the fabricated LPDA are given in Table I.

III. Parametric Study and Analysis

Parametric analysis is performed to investigate the effects of dipole length, width and distance between the elements on antenna return loss and bandwidth using ANSYS HFSS 3D EM simulation software. In this analysis, one parameter is varied while keeping other parameters constant.

A. Variation of Feed Line Width

The feed line width affects the input match of the antenna and is matched to an impedance of 50 Ohms. The variation in width is performed in steps of 0.5 mm and return loss is shown in Fig. 3. The variation of return loss is not considerable and the overall bandwidth is not varying. Hence, feed line width does not affect the bandwidth to a larger extent.

B. Variation of Distance Between Dipole Elements

The variation of distance between the dipoles is studied by considering the distance between the fourth and fifth dipole elements. This is considered as it is the smallest distance and hence, the interaction between these two dipoles would be high. This also affects the length of thee dipoles as mutual coupling between the elements increases with closely spaced dipoles. It is observed that there is an improvement in the return loss at 1.5 GHz and 2 GHz as shown in Fig. 4. However, bandwidth is almost same for all the values of d_4.

C. Variation of Length Ly_1 and Ly_2

The length L_{y1} is length of the lowest frequency dipole elements. The first dipole element is shaped along with other

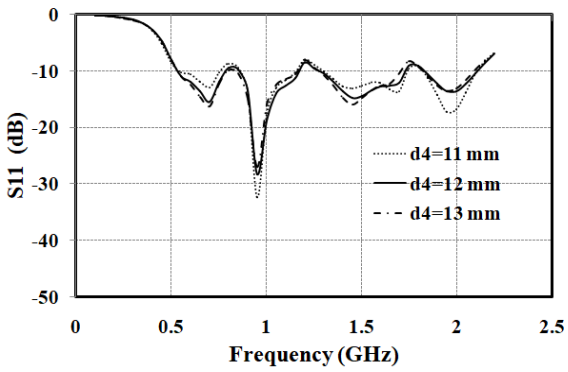

Fig. 4. Simulated S11 for variation in d_4 of the antenna.

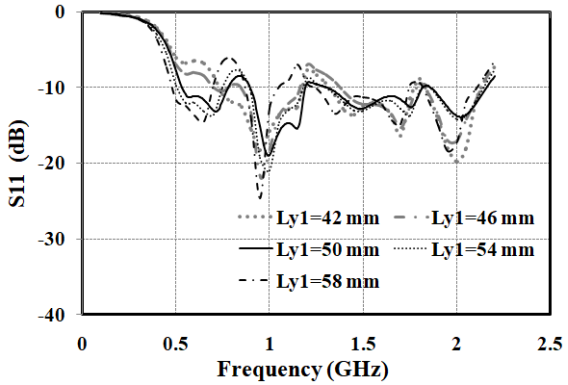

Fig. 5. Simulated S11 for variation in Ly_1 of the antenna.

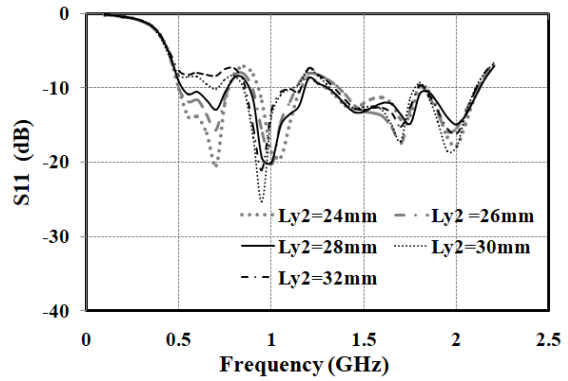

Fig. 6. Simulated S11 for variation in Ly_2 of the antenna.

dipole elements to fit the antenna into a compact size. The length L_{y1} and L_{y2} act as coupled lines due to which the effective electrical length of both the dipoles increases without increasing the physical lengths of the elements. The increase in electrical length results in improvement of the return loss of the antenna array at lower frequencies. It is observed from the variation of L_{y1} that the return loss bandwidth is increasing at the lower frequency range and the variation of L_{y2} causes the return loss to improve by providing better matching at lower frequencies as can be observed from Fig. 5 and Fig. 6.

D. Variation of Length Ly_5

The length of the fifth dipole is considered as the return loss characteristics of the LPDA is poor at mid-band and 2 GHz. As discussed earlier, the largest dipole affects the lowest frequency and smallest dipole affects highest frequency. Hence, the lengths of the middle elements would affect the return

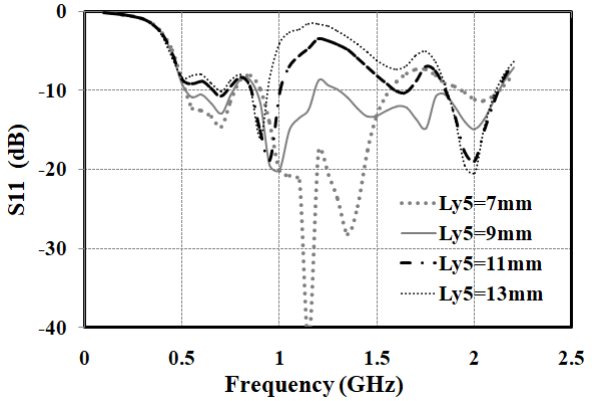

Fig. 7. Simulated S11 for variation in Ly_5 of the antenna.

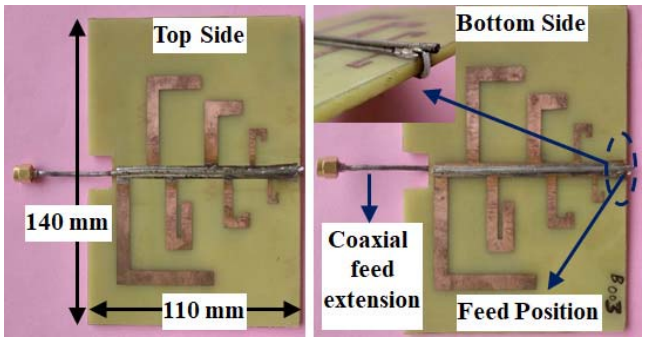

Fig. 8. Top and bottom side of the fabricated LPDA antenna prototype. (inset picture shows feed position).

loss at mid-band frequencies of the antenna. The fifth element affects the return loss the most which can be observed from the return loss plots shown in Fig. 7. The return loss in the mid region is drastically affected even though there is no variation in the lower frequencies regions.

IV. Measured Antenna Results and Discussion

The simulations are validated with a fabricated prototype of LPDA antenna and experimentally tested. The fabricated LPDA prototype antenna is shown in Fig. 8. The coaxial feed is manually soldered across both ends of the feed line with center conductor soldered to top structure and outer conductor is soldered to the bottom structure. The coaxial feed is extended towards the largest dipole from feed point to reduce interference in the radiation pattern of the antenna. The measured and simulated return loss of LPDA UHF sensor is shown in Fig. 9.

The measurements are carried out using HP8719A vector network analyzer. The proposed antenna meets the specification of S11 < -10 dB over 0.5 GHz - 2.2 GHz frequency range. The measured 10 dB return loss bandwidth of the designed antenna is 126%. The simulated results are closely matching the measurement results validating the taper design and lengths of the dipole elements.

The simulated and measured radiation patterns are compared and shown in Fig. 10 (a-e). The E-plane and H-plane patterns have been measured at 0.7 GHz, 1 GHz, 1.5 GHz, 2 GHz and 2.2 GHz respectively. The patterns could not be measured at the lowest frequency i.e. 0.5 GHz due to non availability of the anechoic chamber at that frequency. The E-plane radiation pattern for the above measured frequencies

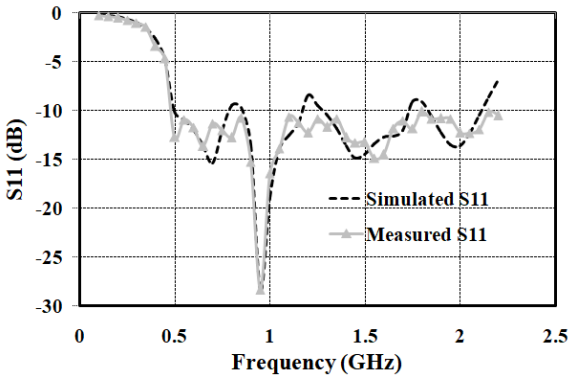

Fig. 9. Simulated and measured S11 of the antenna.

is a directional pattern and the beam width is also sufficient to capture the partial discharges in transformers. The slight variations in the measured and simulated back lobe patterns of the antenna are due to interference caused by coaxial cable feeding the antenna.

The gain of the antenna is measured in an anechoic chamber using gain transfer method wherein two sets of received power measurements are performed for standard antenna (P_{Std}) and prototype test antenna (P_{AUT}). The gain of the prototype test antenna (G_{AUT} in dB) is obtained as G_{std}(dB) + P_{AUT}(dBm) - P_{Std}(dBm). The reference antenna used in the radiation pattern and gain measurement is bi-conical antenna EM-6917B-2 (26MHz – 3GHz). The measured gain of the antenna is -1 to 4.3 dBi over 0.7 – 2.2 GHz with almost flat gain of 4 dBi from 0.8 – 2.2 GHz and is shown in Fig. 11. Within this bandwidth, the effective antenna height is higher than 15 mm as shown in Fig. 12. The designed antenna is compared with other recent reported structures to show its effectiveness in table I. The comparison is with respect to frequency range, fractional bandwidth, antenna size, return loss, gain and effective antenna height.

Though, the published works in [16], [18], [22], and [25] exhibit slightly higher fractional bandwidth compared with proposed antenna but they occupy an area 2.3 times larger than 0.31 λ_0^2. The highest fractional bandwidth among the compared antennas is exhibited by [21] and [25], but it also occupies the largest area among the compared antennas (i.e. 7.1 and 46 times the proposed antenna, respectively). The gain characteristics of the proposed antenna is flat compared to [18] wherein gain varies over a wide range leading to variations in the voltage measurement for different frequencies. Though, [7] and [20] proposes a compact antenna (0.41 λ_0^2 and 0.25 λ_0^2), the fractional bandwidth of the antenna are 88% and 100%, respectively when compared to 126% for the proposed antenna. When comparing the antenna dimension the center frequency is used for calculating λ_0. The proposed antenna also achieves an antenna height of 15 mm (0.7 – 2.2 GHz) which is better than antenna height of 13 mm (0.8 - 1.8 GHz) and 8 mm (0.5 - 1.5 GHz) presented in [7] and [20] showing the effectiveness and higher sensitivity of the proposed design.

V. Partial Discharge Experiment and Results

The designed LPDA UHF antenna is used as a proof of concept for detection of PD's like corona defect, particle

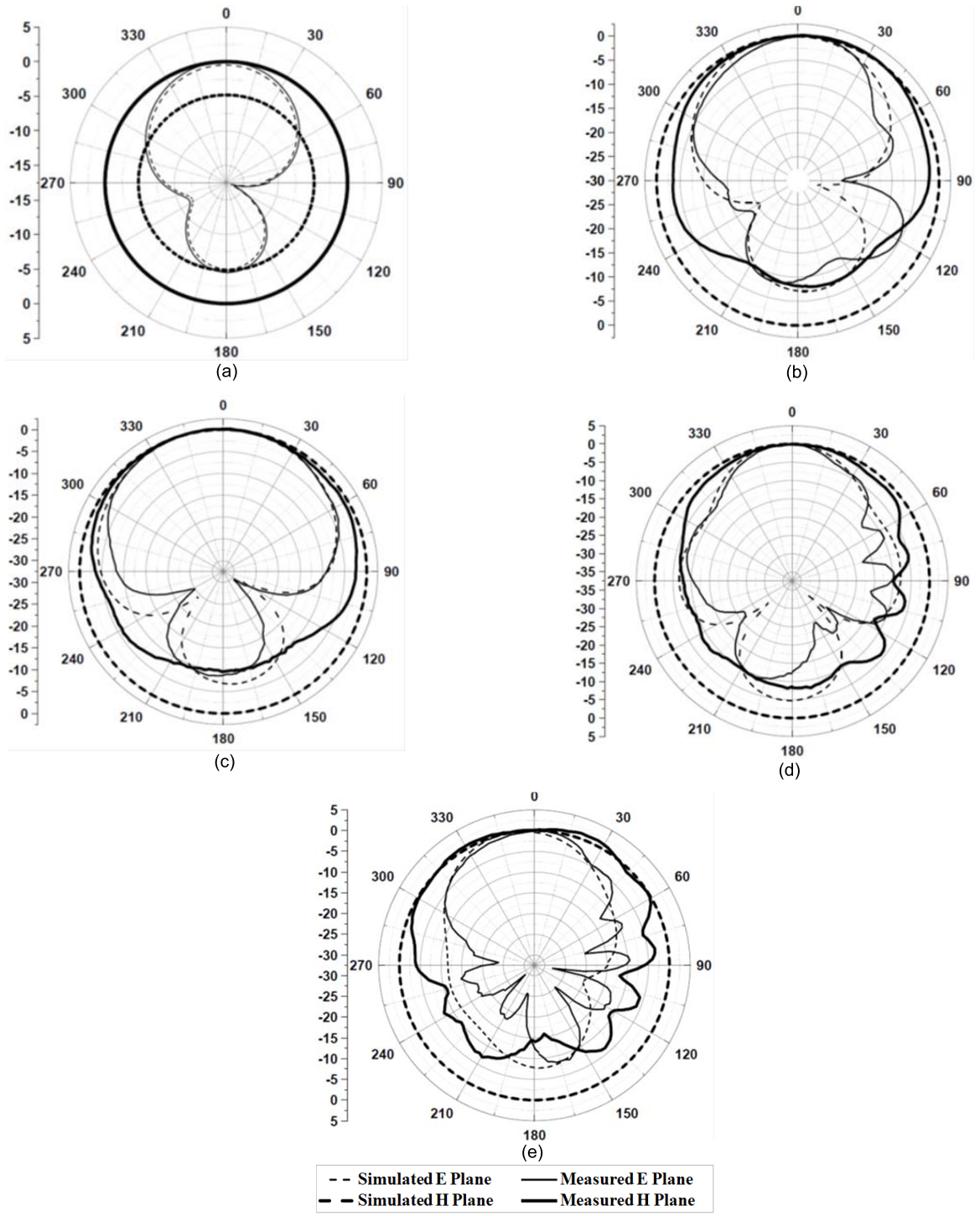

Fig. 10. Simulated and measured radiation patterns for the fabricated antenna (a) 0.7 GHz (b) 1 GHz (c) 1.5 GHz (d) 2 GHz (e) 2.2 GHz.

movement defect, free particles defect and surface defect. The corresponding frequency range of the above PD defects falls between 0.5 - 2.2 GHz.

The block diagram and the experimental set-up of PD detection by the designed LPDA UHF sensor are shown in Fig. 13(a). The test cell used for measurement consists of top and bottom electrodes filled with transformer oil in a cylindrical Perspex tube as shown in Fig 13 (b). The particle movement discharge test cell has 25 mm diameter aluminum sphere and a 2 mm diameter aluminum ball is kept on a 55 mm bottom with slightly concave plane having a 1 cm gap between the two electrodes. The test cell of corona discharge has a top copper needle attached to aluminum rod having radius of curvature of 40 μm and 50 mm bottom aluminum circular plane has a gap of 1 cm between both electrodes. The test cell for free metal particles discharge has a 25 mm diameter top aluminum sphere and 55 mm slightly concave plane having a 1 cm gap between the two electrodes. Inside the test cell, two different particles i.e. 2 mm aluminum ball and copper bead on the bottom electrode are placed. The test cell for

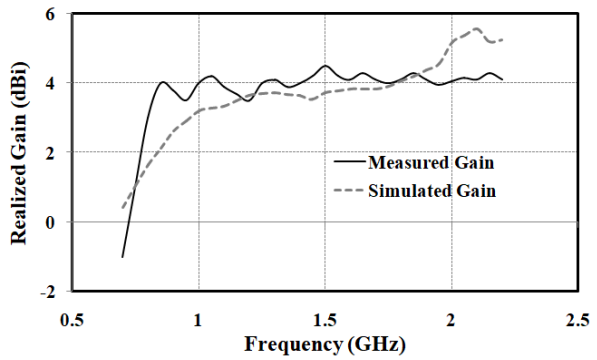

Fig. 11. Simulated and measured realized gain of the proposed LPDA antenna.

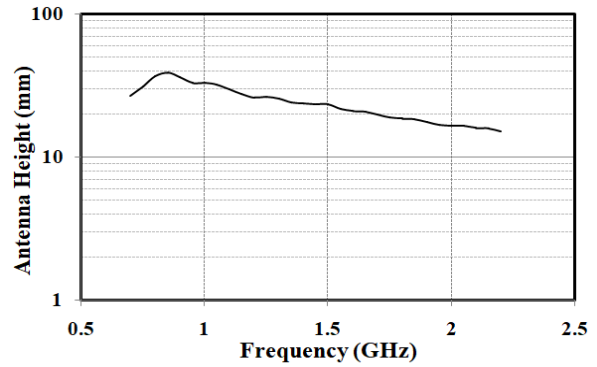

Fig. 12. Effective height of the proposed LPDA antenna.

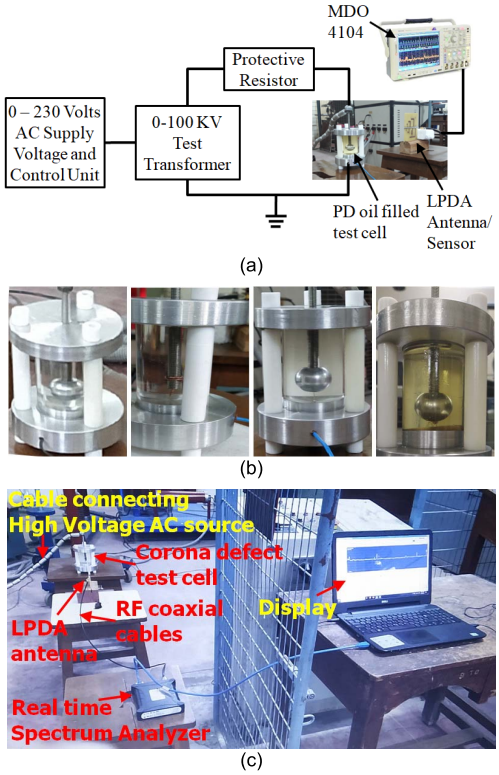

Fig. 13. (a) Block diagram of the PD test system using oscilloscope (b) PD test cells (particle movement, corona, free metal particle and surface defect test cells respectively) (c) PD experimental set-up for antenna in lab using spectrum analyzer.

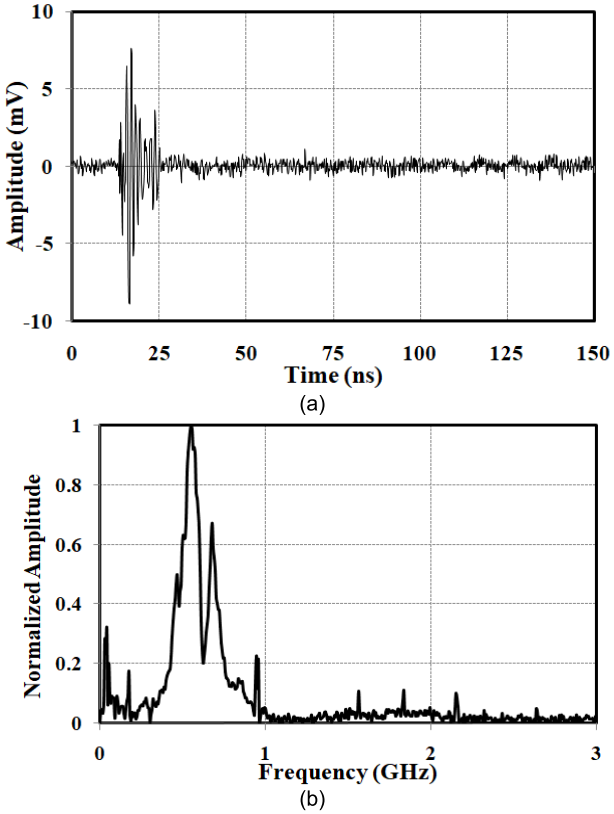

Fig. 14. Particle movement defect at an inception voltage of 7.6 kV in transformer oil (a) Time domain (b) Normalized FFT of UHF signal.

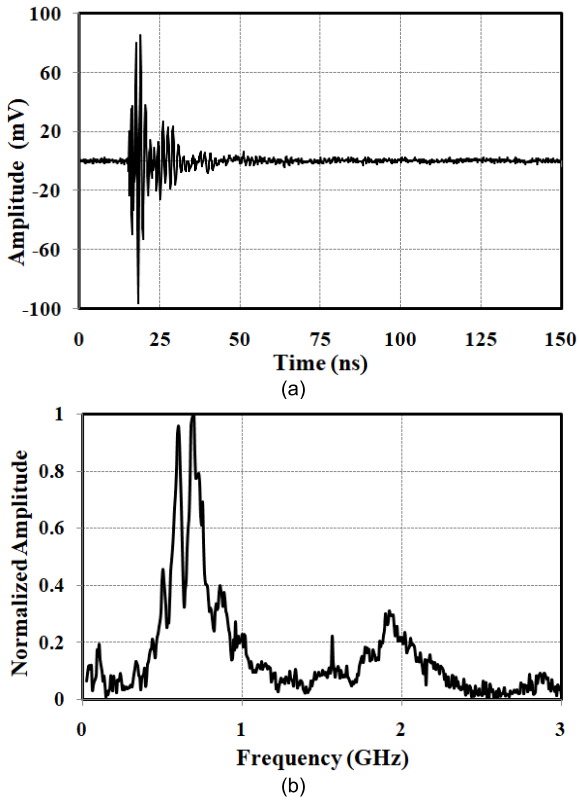

Fig. 15. Corona defect at an inception voltage of 8.7 kV in transformer oil (a) Time domain UHF signal (b) Normalized FFT of UHF signal.

surface discharge has 25 mm diameter aluminum top sphere and 55 mm bottom slightly concave plane having 1 cm gap. Inside the test cell, a pressboard of 5 cm diameter and 2 mm thickness is placed between the two electrodes.

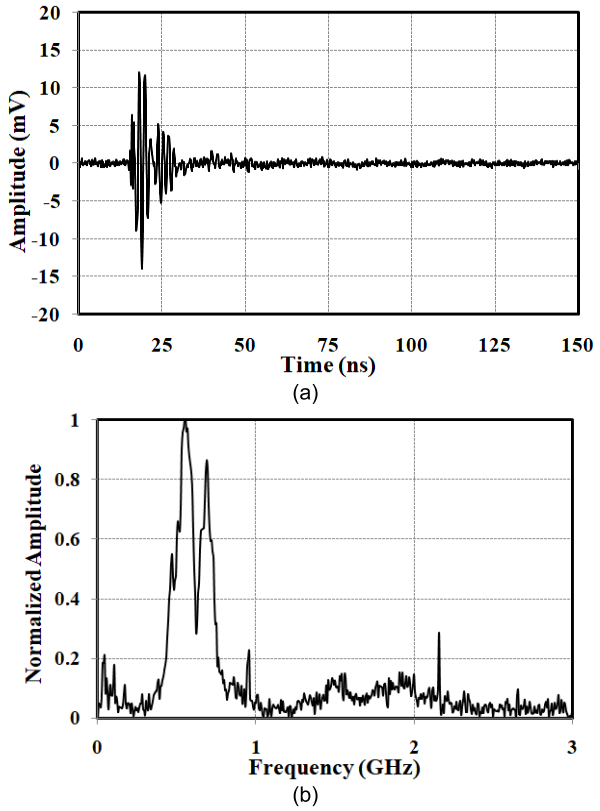

Fig. 16. Free metal particles defect (aluminium ball and copper bead) at an inception voltage of 10.6 kV in transformer oil (a) Time domain UHF signal (b) Normalized FFT of UHF signal.

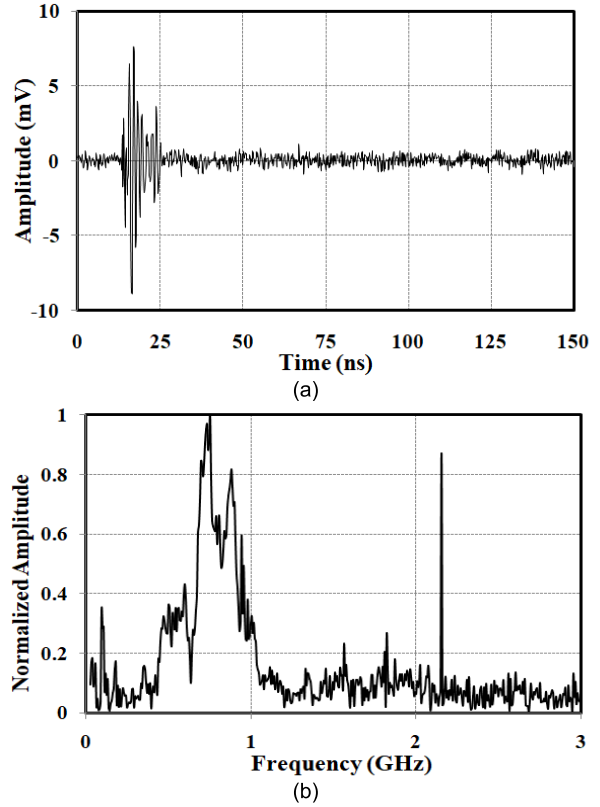

Fig. 17. Surface defect at an inception voltage of 11.8 kV in transformer oil (a) Time domain UHF signal (b) Normalized FFT of UHF signal.

The four PDs i.e. particle movement, Corona, free metal particles and surface discharges are generated at 7.6 kV, 8.7 kV, 10.6 kV and 11.8 kV, respectively. The antenna is placed at a distance of 1m to capture the PD signals. These signals are then viewed in oscilloscope or spectrum analyzer as shown in Fig. 13(c).

Fig. 14 (a) & (b) shows the UHF time domain signal and the respective Fast Fourier Transform (FFT) of the particle movement discharge and its characteristic frequency covers from 0.5 - 1 GHz. The time and frequency domain signals of corona discharge are shown in Fig. 15 (a) & (b) and its characteristic dominant frequency contents lies in 0.4-0.8 GHz. It is observed from Fig. 16 (a) & (b) the dominant frequency signals of free particles discharges are from 0.5 - 0.85 GHz and at 1.6 GHz. The characteristic frequency contents of the surface discharges lies in the range of 0.1 - 1 GHz, 1.6 GHz and 2.1 GHz as shown in the Fig. 17 (a) & (b). The PD experiment result reveals that the designed LPDA UHF sensor is capable of detecting the four different incipient discharge signals with oil filled test object.

VI. Conclusion

A broadband log periodic printed dipole array antenna is presented in this paper. The bandwidth is achieved by optimizing lengths of selected dipole elements and shaping them to provide additional capacitance and effectively reducing the length of the dipole elements. The antenna achieves a fractional bandwidth of 126% within a compact size of 110 mm × 140 mm. The characteristics of the designed LPDA UHF sensor are simple planar design, light weight and broad bandwidth making it useful for measurement of partial discharges. This antenna is designed to detect different types of PD defects occurrences generally falling in the 0.5 - 2.2 GHz frequency range which are detected in power transformer. The proposed antenna is effective in measuring the discharges as it exhibits better antenna height and flat gain performance.

References

[1] P. J. Moore, I. E. Portugues, and I. A. Glover, "Partial discharge investigation of a power transformer using wireless wideband radio-frequency measurements," *IEEE Trans. Power Del.*, vol. 21, no. 1, pp. 528–530, Jan. 2006.

[2] *Capacitive Couplers for UHF Partial Discharge Monitoring*, Nat. Grid Company plc, London, U.K., 1997.

[3] E. Al AlMazam *et al.*, "Partial discharge and oil quality monitoring using an RF antenna," *IEEE Ind. Appl. Mag.*, vol. 16, no. 3, pp. 57–59, Apr. 2010.

[4] A. H. El-Hag *et al.*, "Multi-purpose RF antenna for partial discharge and oil quality monitoring," in *Proc. 3rd Int. Conf. Electr. Power Energy Convers. Syst.*, Istanbul, Turkey, Oct. 2013, pp. 1–5.

[5] A. M. Ishak, M. T. Ishak, M. T. Jusoh, S. F. S. Dardin, and M. D. Judd, "Design and optimization of UHF partial discharge sensors using FDTD modeling," *IEEE Sensors J.*, vol. 17, no. 1, pp. 127–133, Nov. 2017.

[6] J. Lopez-Roldan, T. Tang, and M. Gaskin, "Optimization of a sensor for onsite detection of partial discharges in power transformers by the UHF method," *IEEE Trans. Dielectr. Electr. Insul.*, vol. 15, no. 6, pp. 1634–1639, Dec. 2008.

[7] C. Zachariades, R. Shuttleworth, and R. Giussani, "A dual-slot barrier sensor for partial discharge detection in gas-insulated equipment," *IEEE Sensors J.*, vol. 20, no. 2, pp. 860–867, Jan. 2020.

[8] Q. Wu, G. Liu, Z. Xia, and L. Lu, "The study of Archimedean spiral antenna for partial discharge measurement," in *Proc. 4th Int. Conf. Intell. Control Inf. Process. (ICICIP)*, Beijing, China, Jun. 2013, pp. 694–698.

[9] J. Li, "Hilbert fractal antenna for UHF detection of partial discharges in transformers," *IEEE Trans. Dielectr. Electr. Insul.*, vol. 20, no. 6, pp. 2017–2025, Dec. 2013.

[10] J. Li, T. Jiang, C. Wang, and C. Cheng, "Optimization of UHF Hilbert antenna for partial discharge detection of transformers," *IEEE Trans. Antennas Propag.*, vol. 60, no. 5, pp. 2536–2540, Mar. 2012.
[11] J. Li, P. Wang, T. Jiang, L. Bao, and Z. He, "UHF stacked Hilbert antenna array for partial discharge detection," *IEEE Trans. Antennas Propag.*, vol. 61, no. 11, pp. 5798–5801, Nov. 2013.
[12] A. H. Zahed *et al.*, "Design of Hilbert fractal antenna for partial discharge detection and classification," in *Proc. 4th Int. Conf. Electr. Power Energy Convers. Syst. (EPECS)*, Sharjah, UAE, Nov. 2015, pp. 1–4.
[13] M. M. O. Harbaji *et al.*, "Design of Hilbert fractal antenna for partial discharge classification in oil-paper insulated system," *IEEE Sensors J.*, vol. 17, no. 4, pp. 1037–1045, Feb. 2017.
[14] N. Hidaka, S. Tsujino, H. Sugama, A. Tsuchiya, T. Ishida, and O. Hashimoto, "A design for significantly improving the measurable sensitivity of LOG-periodic dipole antenna arrays for optical electric field sensors," *Microw. Opt. Technol. Lett.*, vol. 57, no. 6, pp. 1386–1390, Jun. 2015.
[15] Z. Hu, Z. Shen, W. Wu, and J. Lu, "Low-profile log-periodic monopole array," *IEEE Trans. Antennas Propag.*, vol. 63, no. 12, pp. 5484–5491, Dec. 2015.
[16] X. Lu and G.-M. Yang, "Miniaturized log periodic dipole array with complementary split-ring resonators," *Microw. Opt. Technol. Lett.*, vol. 58, no. 9, pp. 2217–2221, Sep. 2016.
[17] A. Mirkamali and P. S. Hall, "Wideband frequency reconfiguration of a printed log periodic dipole array," *Microw. Opt. Technol. Lett.*, vol. 52, no. 4, pp. 861–864, Apr. 2010.
[18] C. Zachariades, R. Shuttleworth, R. Giussani, and T. H. Loh, "A wideband spiral UHF coupler with tuning nodules for partial discharge detection," *IEEE Trans. Power Del.*, vol. 34, no. 4, pp. 1300–1308, Aug. 2019.
[19] W. Zhou, P. Wang, Z. Zhao, Q. Wu, and A. Cavallini, "Design of an archimedes spiral antenna for PD tests under repetitive impulsive voltages with fast rise times," *IEEE Trans. Dielectr. Electr. Insul.*, vol. 26, no. 2, pp. 423–430, Apr. 2019.
[20] X. Han, J. Li, L. Zhang, P. Pang, and S. Shen, "A novel PD detection technique for use in GIS based on a combination of UHF and optical sensors," *IEEE Trans. Instrum. Meas.*, vol. 68, no. 8, pp. 2890–2897, Aug. 2019.
[21] Y. Qi *et al.*, "Design of ultra-wide band metal-mountable antenna for UHF partial discharge detection," *IEEE Access*, vol. 7, pp. 60163–60170, 2019.
[22] G. V. R. Xavier, E. G. da Costa, A. J. R. Serres, L. A. M. M. Nobrega, A. C. Oliveira, and H. F. S. Sousa, "Design and application of a circular printed monopole antenna in partial discharge detection," *IEEE Sensors J.*, vol. 19, no. 10, pp. 3718–3725, May 2019.
[23] J. Chen, J. Ludwig, and S. Lim, "Design of a compact log-periodic dipole array using T-shaped top loadings," *IEEE Antennas Wireless Propag. Lett.*, vol. 16, pp. 1585–1588, 2017.
[24] L. Chang, S. He, J. Q. Zhang, and D. Li, "A compact dielectric-loaded log-periodic dipole array (LPDA) antenna," *IEEE Antennas Wireless Propag. Lett.*, vol. 16, pp. 2759–2762, 2017.
[25] K. Anim and Y.-B. Jung, "Shortened log-periodic dipole antenna using printed dual-band dipole elements," *IEEE Trans. Antennas Propag.*, vol. 66, no. 12, pp. 6762–6771, Dec. 2018.
[26] J. M. Wen, C. K. Wang, W. Hong, Y. M. Pan, and S. Y. Zheng, "A wideband switched-beam antenna array fed by compact single-layer Butler matrix," *IEEE Trans. Antennas Propag.*, vol. 69, no. 8, pp. 5130–5135, Aug. 2021.
[27] K. K. Mistry, P. I. Lazaridis, Z. D. Zaharis, and T. H. Loh, "Design and optimization of compact printed log-periodic dipole array antennas with extended low-frequency response," *Electronics*, vol. 10, pp. 1–10, Jan. 2021.
[28] R. Albarracin, J. A. A. Rey, and A. A. Masud, "On the use of monopole antennas for determining the effect of the enclosure of a power transformer tank in partial discharges electromagnetic propagation," *Sensors*, vol. 16, pp. 1–17, Feb. 2016.
[29] J. Du *et al.*, "Investigation on the propagation characteristics of PD-induced electromagnetic waves in an actual 110 kV power transformer and its simulation results," *IEEE Trans. Dielectr. Electr. Insul.*, vol. 25, no. 5, pp. 1634–1639, Oct. 2018.
[30] R. Carrel, "The design of log-periodic dipole antennas," in *Proc. IRE Int. Conv. Rec.*, New York, NY, USA, Mar. 1966, pp. 61–75.

Meka Kalyan Chakravarthi received the B.Tech. degree in electrical and electronics engineering from Jawaharlal Nehru Technological University (JNTU), Hyderabad, India, in 2008, and the master's degree in power electronics and power systems from Acharya Nagarjuna University (ANU), Guntur, Andhra Pradesh, India, in 2010. He is currently pursuing the Ph.D. degree with the Department of Electrical Engineering, NIT Warangal. His research interests include condition monitoring of power transformers, ultra high frequency sensors, and high voltage engineering.

A. V. Giridhar (Senior Member, IEEE) received the Doctorate degree from IIT Madras in 2011. He joined the National Institute of Technology, Warangal, India, in 2012, where he is currently an Assistant Professor with the Department of Electrical Engineering. He is also working on SPARC Project as a Co PI. Also, he had done consultancy services to state power utility. He has published more than ten articles in journals and conferences. His research area includes high-voltage engineering, condition monitoring and diagnosis of high voltage power apparatus, pulsed power technology, and nano dielectrics.

Gande Arun Kumar (Senior Member, IEEE) received the B.E. degree in electronics and communications engineering from Osmania University (OU), Hyderabad, India, in 2004, and the M.E.Tel.E. and Ph.D. degrees from Jadavpur University (JU), Kolkata, West Bengal, India, in 2006 and 2012, respectively. He joined the Circuits and Systems Division, Society for Applied Microwave Electronic Engineering and Research (SAMEER), Kolkata, India, under the Ministry of Electronics and Information Technology (Meity), Government of India, in 2010, and worked as a Scientist-B from August 2010 to March 2014 and a Scientist-C from April 2014 to May 2018. In June 2018, he joined the Electronics and Communications Engineering Department, NIT Warangal, Telangana, where he is currently an Assistant Professor. He has published more than 38 articles in journals and conferences. He has successfully completed two projects sponsored by DRDO and more than ten projects sponsored by Meity. His research interests include microwave and millimeter wave passive and active circuits, metamaterials, substrate integrated waveguides, and reconfigurable filters, and ultra-high frequency sensors. He is a Life Member of IETE and the Society of EMC Engineers, India. He received the DST-SERB-Early Career Research Award in 2019.

D. V. S. S. Siva Sarma (Senior Member, IEEE) received the B.Tech. degree in EEE and the M.Tech. degree in power systems from the JNTU College of Engineering, Anantapur, in 1986 and 1988, respectively, and the Doctorate degree from IIT Madras in 1993. He is currently a Professor with the Department of Electrical Engineering. He is also actively doing consultancy services for state irrigation departments of Andhra Pradesh and Telangana. He published more than 75 articles in journals and conferences. His areas of interest include power system transients, power quality, protection and condition monitoring of power apparatus, and EMTP applications. He received the IEEE Outstanding Branch Counselor and Advisor Award in 2009. He worked as the Chair of Student Activities for the IEEE Hyderabad Section from 2009 to 2011, and the Vice-Chair and the Chair of the PES/IAS/PELS Joint Chapter, IEEE Hyderabad Section, in 2011 and 2012. He is also serving as the Chairperson for the IEEE Education Society Chapter of Hyderabad Section.